ADVANCING EARTH AND SPACE SCIENCES

Water Resources Research

RESEARCH ARTICLE
10.1029/2023WR034813

Linking Sediment and Water Column Phosphorus Dynamics to Oxygen, Temperature, and Aeration in Shallow Eutrophic Lakes

A. P. Kirol[1], A. M. Morales-Williams[2], D. C. Braun[3], C. L. Marti[4], O. E. Pierson[5], K. J. Wagner[6], and A. W. Schroth[1,2]

[1]Department of Geography and Geosciences, University of Vermont, Burlington, VT, USA, [2]Rubenstein School of Environment and Natural Resources, University of Vermont, Burlington, VT, USA, [3]Stone Environmental, Inc., Montpelier, VT, USA, [4]School of Engineering, The University of Western Australia, Perth, WA, Australia, [5]Vermont Department of Environmental Conservation, Montpelier, VT, USA, [6]Water Resources Services, Wilbraham, MA, USA

Key Points:

- Legacy phosphorus mobility was driven by either episodic wind-mediated mixing or seasonal turnover in two proximal shallow eutrophic systems
- Aeration altered hydrodynamics to change from seasonal to wind-driven internal loading of legacy phosphorus, but it was not suppressed
- Heterogeneous spatiotemporal controls on internal legacy phosphorus loading present challenges to achieving water quality goals

Supporting Information:

Supporting Information may be found in the online version of this article.

Correspondence to:

A. P. Kirol,
ashton.kirol@gmail.com

Citation:

Kirol, A. P., Morales-Williams, A. M., Braun, D. C., Marti, C. L., Pierson, O. E., Wagner, K. J., & Schroth, A. W. (2024). Linking sediment and water column phosphorus dynamics to oxygen, temperature, and aeration in shallow eutrophic lakes. *Water Resources Research*, *60*, e2023WR034813. https://doi.org/10.1029/2023WR034813

Received 3 MAR 2023
Accepted 22 DEC 2023

Author Contributions:

Conceptualization: A. P. Kirol, A. M. Morales-Williams, C. L. Marti, K. J. Wagner, A. W. Schroth
Formal analysis: A. P. Kirol
Funding acquisition: A. M. Morales-Williams, D. C. Braun, C. L. Marti, O. E. Pierson, A. W. Schroth
Investigation: A. P. Kirol, A. W. Schroth
Methodology: K. J. Wagner, A. W. Schroth

Abstract Water quality improvements in shallow eutrophic lakes are commonly delayed due to loading from legacy phosphorus (P)-enriched sediments, even with reduced external nutrient loads. It is critical to understand the drivers of internal P loading to suppress or remove this source of P and meet water quality goals. We contrast the drivers of internal P loading in two shallow eutrophic systems (Lake Carmi and Missisquoi Bay). Legacy P dynamics in the unmanipulated systems were compared to Lake Carmi during aeration. In-situ high frequency water column monitoring along with water and sediment sampling was used to study P dynamics in response to changing lake conditions and aeration. Despite both systems exhibiting P mobility controlled by iron redox cycling, we observed distinct differences in the spatial extent and drivers of internal P loading. Legacy P loading was controlled by seasonal drivers in Lake Carmi, but by spatially variable and highly transient wind driven forcing of hydrodynamics in Missisquoi Bay. Aeration altered the mixing regime of Lake Carmi and shifted loading dynamics to frequent wind-driven pulses of legacy P to surface waters akin to those of Missisquoi Bay. Mean hypolimnetic dissolved oxygen increased with aeration, but greater oxygen demand rates and periods of anoxia under transient stratification still resulted in internal P loading. Surface P concentrations were higher in summer months with aeration compared to previous years. This research illustrates the dynamic nature of legacy P behavior within and between shallow eutrophic lakes and the challenges in addressing this common water resources threat.

Plain Language Summary Shallow lakes with high amounts of nutrients like phosphorus often experience worsening water quality and harmful algae blooms. Even if less phosphorus enters the lake from the watershed, phosphorus already in the lake can cycle between the water and sediment for decades. It is important to understand how phosphorus moves within lakes to make management decisions. We studied what causes the release of phosphorus from sediment in Lake Carmi and Missisquoi Bay, Lake Champlain. These observations were compared to Lake Carmi during 4 years of whole-lake aeration designed to limit phosphorus release. We found that the release of phosphorus at both study sites was tied to chemical reactions of iron. The timing of this release was controlled by seasonal changes in Lake Carmi before aeration, and by frequent wind-driven mixing in Missisquoi Bay. Aeration changed the timing of mixing in Lake Carmi but did not decrease the amount of phosphorus recycled from the sediment. Aeration also increased the rate of oxygen consumption in Lake Carmi which quickly led to phosphorus release during periods of calm wind. This research shows the highly dynamic nature of phosphorus behavior within shallow lakes which is important to understand when making management decisions.

1. Introduction

Phosphorus (P) mobility is one of the most important water quality drivers in freshwater lakes because P is essential for growth of all biota. High nutrient loading, however, often results in eutrophication by causing elevated phytoplankton biomass, oxygen depletion, and amplification of ecosystem processes (Birk et al., 2020; Heisler et al., 2008; Paerl et al., 2020). Human activities have dramatically increased the rate of nutrient pollution worldwide through waste disposal, stormwater runoff, agriculture, and atmospheric inputs (Glibert, 2020). Thus,

Project Administration: A. M. Morales-Williams, D. C. Braun, C. L. Marti, O. E. Pierson, A. W. Schroth
Resources: O. E. Pierson, A. W. Schroth
Software: C. L. Marti
Supervision: A. M. Morales-Williams, D. C. Braun, A. W. Schroth
Visualization: A. P. Kirol, C. L. Marti
Writing – original draft: A. P. Kirol
Writing – review & editing: A. M. Morales-Williams, D. C. Braun, C. L. Marti, O. E. Pierson, K. J. Wagner, A. W. Schroth

anthropogenic eutrophication is the one of the most ubiquitous global water quality problems that societies have struggled to address (Schindler, 2012).

Targeted efforts to suppress P inputs into lakes have sometimes been successful, but improvements in lake conditions are often reduced or delayed due to a positive feedback loop of internal P loading, which recycles soluble P from lake sediments into the water column (Jeppesen et al., 2005; Marsden, 1989). The historical buildup of P in lake sediments (legacy P) represents a large nutrient pool which can significantly increase the time required for water quality improvements after external nutrient inputs like agricultural runoff are reduced by watershed management efforts. Legacy P contributes to initiating and sustaining cyanobacteria blooms in shallow polymictic systems where it can be transported to the photic zone through frequent water column mixing and sediment resuspension (Giles et al., 2016; Håkanson, 2004; Sondergaard et al., 2001). Certain cyanobacteria can also initiate growth at the sediment water interface (SWI), and legacy P released from the sediment supports this growth without the need for mixing (Carey et al., 2009; Cottingham et al., 2015). Internal P loading is a larger problem in shallow systems where frequent mixing or early fall turnover makes those nutrients available during more favorable light and temperature conditions for cyanobacteria blooms in temperate climate zones.

A variety of interrelated chemical, biological and physical processes control the exchange of P between lake sediments and the water column (Boström et al., 1988; Wetzel, 2001). P can be remobilized through the desorption of orthophosphate bound to particles in the sediment, dissolution of P containing minerals, mineralization of organic matter during oxygenated conditions, or ligand exchange including phosphate-hydroxide ion exchange (Giles et al., 2015; Orihel et al., 2017; Søndergaard et al., 2003). Redox-driven Fe cycling is a dominant mechanism of P sequestration and release from sediments in many shallow eutrophic lakes, but other geochemical drivers have been found to play an important role in P cycling in some systems including pH, alkalinity, iron mineral speciation, remineralization of organics, and nitrate or sulfate concentrations (Giles et al., 2016; Katsev et al., 2006; Smith et al., 2011; Wetzel, 2001).

Internal P loading from the release of phosphate adsorbed to redox-sensitive Fe minerals in the surface sediment under reducing conditions has been identified as a significant source of nutrients in many shallow eutrophic lakes (Giles et al., 2016; Mortimer, 1941; Petticrew & Arocena, 2001; Søndergaard et al., 2013; Tammeorg et al., 2020). Reducing conditions are common at the SWI due to anoxia that develops in the hypolimnion when lakes thermally stratify in the summer. The severity and duration of hypolimnetic anoxia varies between lakes due to many factors including morphometry, climate, and trophic status (Snortheim et al., 2017; Trolle et al., 2011). Oxygen is consumed by the decomposition of organic matter at the sediment surface and by the chemical oxidation of reduced compounds in the sediment (Beutel et al., 2007; Bowman & Delfino, 1980; Müller et al., 2012). Hypolimnetic oxygen demand depends on a lake's productivity, hypolimnetic depth, dissolved oxygen (DO) concentration overlying the SWI, and oxygen diffusion rates at the SWI (Müller et al., 2012). The oxygen depletion rate (ODR) can vary from low (<0.01 mg/L/day) to rapid rates of depletion (>2 mg/L/day) (Burns, 1995; Rhodes et al., 2017).

Low DO at the SWI can cause the reductive dissolution of iron oxide minerals that commonly immobilize P in sediment (Orihel et al., 2017; Schroth et al., 2015). During this process, phosphate is released into sediment pore water where it can be incorporated into various mineral phases or enter the bottom water through diffusion or advection (Pettersson, 1998; Wetzel, 2001).

Mitigating the effects of P pollution often requires internal P loading suppression in addition to reducing nutrient inputs from the watershed (Bormans et al., 2016; Jilbert et al., 2020). Studies show that as much as 40%–80% of total in-lake P in summer months can come from internal loading, disproportionately contributing to fluxes in summer months when warm, stable conditions favor cyanobacteria bloom development (James, 2017; Song et al., 2017; Steinman et al., 2009; Zia et al., 2022). It has been estimated that in some systems, P released from sediments can support up to 74% of phytoplankton P demand at times (Cowan & Boynton, 1996). Suppressing internal P loading from legacy P sources is therefore a critical component of mitigating cyanobacteria blooms in shallow eutrophic lakes. There are many available management options, and selecting the proper intervention relies on assessing a variety of physical and chemical factors within each lake as well as on accurately quantifying internal P loading (Castelletti et al., 2010; Lürling & Mucci, 2020; Robertson & Diebel, 2020). Physical and chemical in-lake intervention methods have previously been implemented in eutrophic lakes to suppress internal P loading. These include water column aeration (artificial mixing or circulation), hypolimnetic withdrawal, chemical P inactivation (sediment-P binding), and sediment dredging (Cooke et al., 2016; Jilbert et al., 2020;

Wagner, 2017). Reaching in-lake P goals relies on understanding interrelated physical and biogeochemical processes, and how these processes are altered through lake restoration actions.

Our objective in this study was to assess the effects of both unmanipulated and manipulated dynamic water column conditions on internal P loading to help inform future management efforts that target this ubiquitous water pollution problem. We used a combination of high frequency in-situ monitoring and spatially and temporally targeted water and sediment sampling to quantify P mobility in a dimictic lake (Lake Carmi) before and during an aeration intervention, and in a shallow polymictic embayment (Missisquoi Bay) where legacy P suppression is being considered as a management strategy. This novel monitoring framework captured changes in water column dynamics and P mobility in response to aeration and weather conditions over short time scales. Our research questions centered around how the drivers of internal P loading differed between these two shallow systems, and how suppression methods could be used to target those specific drivers.

We hypothesized that differences in hydrodynamics control the spatial and temporal distribution of internal P loading events between Lake Carmi and Missisquoi Bay. Most of the internal P loading in Lake Carmi is expected to occur in the deep central trough associated with the dissolution of Fe species triggered by anoxia during seasonal stratification. Legacy P availability is then controlled by the timing of seasonal turnover which brings nutrients in the hypolimnion to the surface. Because of this, aeration during the summer and fall will promote water column mixing and maintain bottom water DO in the deepest segments of Lake Carmi, decoupling Fe and P behavior. In contrast to Lake Carmi, Missisquoi Bay is a polymictic system that does not experience sustained hypolimnetic anoxia but does have significant internal loading during periods of transient stratification (Giles et al., 2016). We predicted that there are distinct hot spots of potentially labile legacy P in Missisquoi Bay driven by the co-location of zones of high sediment deposition in the deepest segments and frequent, albeit transient, anoxia that triggers most of the internal P loading within the bay. Legacy P is brought to the surface in pulses due to the shallow depth and frequent wind-driven mixing of the bay. This unique combination of high frequency, long term and geospatial data sets provides novel insight into the temporal and spatial dynamic nature of internal P loading in shallow systems and illustrates the complexities in heterogeneous and site-specific drivers of internal P loading that must be considered when assessing the capacity to suppress the release of legacy P from lake sediments.

2. Materials and Methods

2.1. Study Sites

Lake Carmi is a relatively shallow (4 m mean depth, 10 m maximum depth) dimictic eutrophic lake in Franklin, VT (Figure 1). It has a surface area of 5.7 km^2 and a watershed of 31.2 km^2, giving it a catchment to lake area ratio (A_C:A_L) of nearly 5.5 (VT ANR, 2008). Marsh Brook and several small tributaries flow into Lake Carmi which then drains into the Pike River to the northeast. Tilled/untilled farmland or agricultural pasture makes up 21% of the watershed (VT DEC, 2020).

In 2008, when a total maximum daily load (TMDL) for Lake Carmi was developed, a target concentration of 22 μg/L total phosphorus (TP) was issued relative to the annual average of 28 μg/L derived from long-term monitoring data (VT ANR, 2008). Mean TP has increased to ∼34 μg/L in the last decade (Schroth et al., 2021). Cyanobacteria blooms were first detected in 1976 and have worsened in recent decades. Lake Carmi was listed as an impaired water body under Section 303(d) of the Federal Clean Water Act in 2009 and was designated as Vermont's first Lake in Crisis in 2018 under Vermont Act 168 (VT DEC, 2020). In response, the State of Vermont issued a Lake Carmi Crisis Response Plan that targeted multiple P sources within the watershed with a goal of lowering concentrations within the lake. Agricultural land, developed land, wastewater sources, and internal P loading were areas targeted for P reductions. Land use and agricultural practices are a primary driver of long-term eutrophication trends in Lake Carmi, and internal loading of legacy sediment P is thought to be an important driver in the initiation of cyanobacteria blooms (VT ANR, 2008). In 2019, a whole-lake aeration system was installed to maintain oxygenated conditions throughout the lake and suppress the release of sediment bound P. A target threshold of 2.5 mg/L DO at a depth of 8 m was set by the VT DEC. The system consists of two compressors that force air through 80 diffuser disks located on the lake bottom (Figure 1) (VT DEC, 2020). The aeration system is managed by VT DEC, and our group did not manipulate the system design or timing of aeration during this study period.

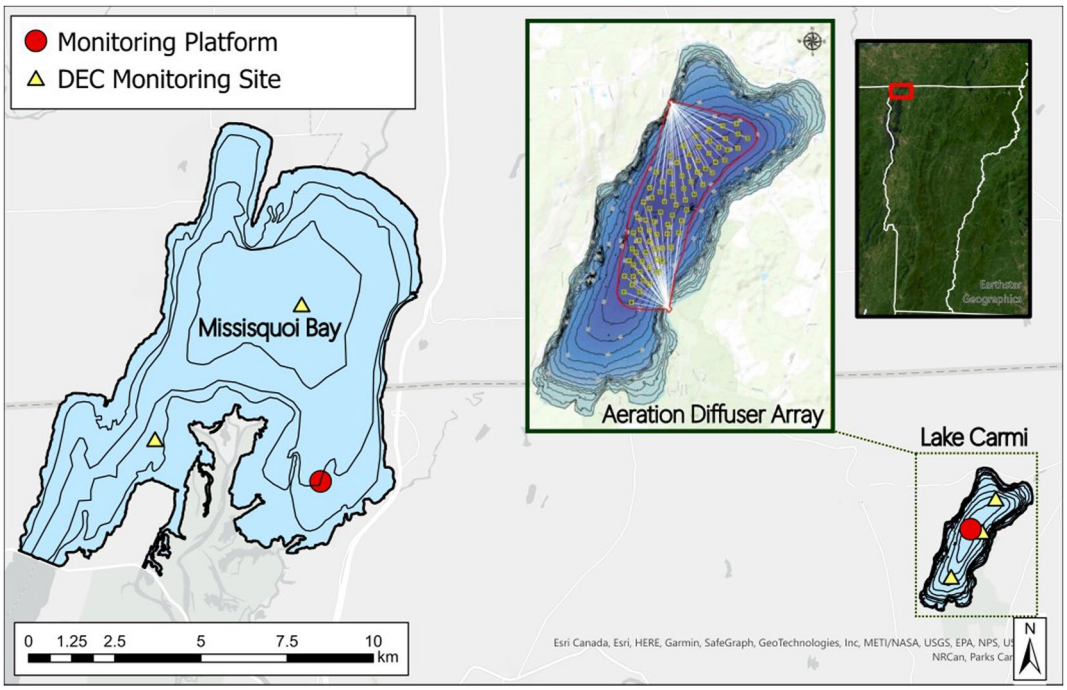

Figure 1. Missisquoi Bay and Lake Carmi along the Northern State of Vermont, U.S.—Canada border. The monitoring sites for this research are marked in red (circles). Vermont Department of Environmental Conservation (VT DEC) long term monitoring sites are marked in yellow (triangles). Bathymetric contour lines at intervals of 1 m are displayed for each study site. The central contour line denotes the depth of 4 m for Missisquoi Bay and the depth of 10 m for Lake Carmi. The inset diagram shows the aeration system installed in Lake Carmi in 2019 which is comprised of two compressors connected to 80 diffuser discs on the lake bottom (Franklin Watershed Committee, 2019).

Missisquoi Bay is a shallow (2.8 m mean depth, 4 m maximum depth) polymictic eutrophic bay in the northeastern-most segment of Lake Champlain (Figure 1) located at the United States - Canada border. It has a surface area of 77.5 km^2 and a watershed of 3,105 km^2, giving it a high A_c:A_L of 40 (Levine et al., 2012; U.S. EPA, 2016). Three main tributaries (the Missisquoi, Pike, and Rock Rivers) flow into Missisquoi Bay and it is connected to the main lake through a small outlet channel to the southwest that was further constricted by the construction of a causeway in 1937 (Mendelsohn et al., 1997). Land cover in the Missisquoi Bay watershed is largely forested or agricultural (62% and 25%–30% respectively) (Levine et al., 2012; Ostrofsky et al., 2020).

Eutrophication increased in the later twentieth century concurrent with agricultural intensification. Total P concentrations average 42 ± 15 μg/L, compared to the EPA TMDL target of 25 μg/L (Levine et al., 2012; Melendez-Pastor et al., 2019). Total P increased by 79% from 1980 to 2009, and cyanobacteria blooms have also increased over that time (Smeltzer et al., 2012). Paleolimnological records of phytoplankton pigments confirm the proliferation of cyanobacteria since the 1970's (Levine et al., 2012). In 2016, the TMDL for Lake Champlain established that P needed to be reduced by 33.7% for the whole lake and 64.3% in Missisquoi Bay specifically (U.S. EPA, 2016). Mass balance studies show that internal P loading accounts for as much as 20% of the annual total P input into Missisquoi Bay and can be anywhere from 50% to 300% of riverine P inputs during summer months (Isles et al., 2015; LimnoTech, 2012; Zia et al., 2022). This fraction can be even higher over short periods of intense internal loading during dry/calm conditions when external loads from runoff are relatively low.

2.2. Monitoring Framework

Beginning in 2018, Lake Carmi was monitored using a combination of high-frequency automated sensors and manual sampling. Sampling occurred in the deep (~9.5 m) central trough that is the focus of aeration intervention which began in 2019. The location was chosen to be in proximity to the VT DEC long-term monitoring station in the central lake which allowed us leverage historical data for comparison to years before 2018. Water column monitoring equipment was deployed from 2018 through 2022 during the summer and fall. Sediment and bottom

water samples were collected in 2020 and 2021 spanning the active aeration period. In addition to our study data, we leverage VT DEC long-term monitoring data that were collected bi-weekly from several depths at three monitoring sites. The monitoring platform was visited every 2 weeks during deployment to collect samples and perform equipment maintenance which coincided with VT DEC sampling events. Data were collected through summer/fall aeration, and the equipment was removed in November, after the last VT DEC sampling event.

Similar monitoring equipment was deployed in Missisquoi Bay for this study in 2020 (July–November) and 2021 (May–November) at a site that has been monitored by our research group at the University of Vermont since 2012 (Giles et al., 2016; Isles et al., 2015). Sediment cores were taken in 2020 spanning the waters within the United States and along the U.S.-Canada border across a series of predetermined transects (Figure S1 in Supporting Information S1). Covid protocols prevented sediment core sampling in Canadian waters in 2020. Samples were collected from all transects of the bay in 2021. In addition to our study sites, there are two Lake Champlain Long-term Water Quality and Biological Monitoring Program (LTMP) monitoring sites in Missisquoi Bay (Figure 1). Station 50 and 53 are located in southwest and central Missisquoi Bay respectively. These sites are monitored in partnership among the Lake Champlain Basin Program, the State University of New York at Plattsburgh, the New York Department of Environmental Conservation, VT DEC, and the EPA (Lake Champlain Long-Term Water Quality and Biological Monitoring Program, 2022).

2.3. Water Column Monitoring

Data collected from Missisquoi Bay and Lake Carmi were used to assess the conditions for legacy P distribution and internal loading. Since 2018, we have maintained a mooring at the Lake Carmi field site equipped with six in-situ water temperature and DO sensors. The sensors are located at approximately 0.15, 0.5, 2, 3, 5, and 7.5 m above the SWI. This vertical resolution in the deepest part of the lake allowed for monitoring of DO and temperature stratification within the water column. High-frequency (15 min) data were recorded on each sensor. Temperature profiles from sensor data were used to calculate Schmidt water column stability (e.g., Giles et al., 2016; Read et al., 2011). Schmidt stability represents the work per unit area required to overcome the potential energy of stratification and thoroughly mix the water column (Idso, 1973; Schmidt, 1928). Estimated ODR were calculated based on data collected by the deepest DO sensor.

In 2020–2022, a monitoring platform was deployed at the Lake Carmi field site to further supplement long-term monitoring efforts. The platform housed an automated ISCO 3700 water sampler (2020–2021), YSI EXO 6 series sonde vertical profiling system, and Onset HOBO RX3000 meteorological station. The ISCO was programmed to collect daily water samples from ~0.5 m above the SWI to capture P released from the sediment during internal loading. Samples were stored within the ISCO in 500 mL high density polyethylene bottles pre-acidified with sulfuric acid following established protocols (Isles et al., 2015). A blank (acidified deionized water) was placed in the ISCO during bi-weekly cycles and collected and analyzed along with lake water samples. Blank concentrations of TP were always less than 10% of water sample concentrations collected by the ISCO.

The vertical profiling system consisted of a YSI multi-parameter water quality Sonde on an automated winch that moves throughout the water column to collect readings. High-frequency (hourly) data were collected at 0.5 m intervals between 0.5 m below the surface and approximately 0.5 m above the sediment. The sonde collected readings of water temperature, DO, pH, turbidity, conductivity, chlorophyll-a, phycocyanin, and sensor depth. The meteorological station housed on the platform measured air temperature, wind speed and direction, relative humidity, and solar radiation at 5-min intervals at 3 m above the surface water.

A similar platform was deployed in the southeast segment of Missisquoi Bay with a vertical profiler and meteorological station. The data collection protocol was the same for these instruments. The water depth at the Missisquoi Bay platform location is approximately 2.5 m. Bottom water samples were collected manually in Missisquoi Bay across several dates and locations to capture low DO events. Samples were taken at ~0.5 m above the SWI using a manual/peristaltic pump. The samples were filtered through a 0.45 μm polyethersulfone filter into trace metal grade acid washed 15 mL vials and then acidified to 1% using concentrated trace metal grade nitric acid.

2.4. Sediment Core Collection

To monitor changing sediment P and related geochemical constituent inventories over time and in response to aeration, triplicate sediment cores were collected monthly from the central monitoring location in Lake Carmi

beginning in May (pre-aeration) through November (post-aeration) in 2020 and 2021. Previous research in Missisquoi Bay shows that the top centimeter of sediment has the largest flux of P due to redox conditions (Smith et al., 2011). Analysis of deeper sediment shows possible flux of P through the sediment profile. Samples were collected manually by gravity core, then stored on ice and shaded from sunlight to limit photochemical reactions until the core was sectioned (<1 hr from collection). Each core was sectioned (0–1 cm, 1–2 cm, 2–4 cm, 4–6 cm, and 6–10 cm intervals), and the respective sections from each core were homogenized. Sediment samples were then weighed and freeze-dried for analysis. Dry sediment bulk density (g/cm^3) was calculated for each sample split as dried sediment mass divided by wet sample volume (Dadey et al., 1992).

Sediment cores were collected across Missisquoi Bay to determine the spatial distribution of P and metals to assess intervention methods. Sites were chosen using a random number generator along predetermined transects across the bay in regions that were modeled to be exposed to low DO conditions at the SWI (Figure S1 in Supporting Information S1). Additional samples were taken from deep areas with predicted high P concentrations and exposure to anoxia. Two cores were collected at each location and sections (0–1 cm, 1–4 cm, and 4–10 cm) were homogenized and freeze dried. A total of 110 sediment cores were collected from Missisquoi Bay including duplicate samples at several locations.

2.5. Laboratory Analysis

Dried sediment samples were analyzed for both total and redox-sensitive P, Fe, and Mn through triplicate extractions. Redox sensitive P and metals were extracted using an ascorbate-citrate-bicarbonate solution described in previous research (Anschutz et al., 1998; Giles et al., 2016; Smith et al., 2011). The samples were then diluted with 1% HCl and analyzed by PerkinElmer Avio 200 inductively coupled plasma optical emission spectrometry (ICP-OES). A separate *aqua regia* digestion was performed to test for total P and metals in the sediment samples (EPA method 3050B; U.S. EPA, 1996). Diluted samples were again analyzed by ICP-OES. Lake Carmi water samples were analyzed for total P and nitrogen (N) at the Vermont Agricultural and Environmental Lab in Randolph, VT, to maintain consistency with ongoing VT DEC nutrient monitoring methods in Lake Carmi. Missisquoi Bay water samples were analyzed for total dissolved P by SEAL AutoAnalyzer 3 HR, and for metals by ICP-OES.

2.6. Data Analysis

A paired *T*-test was used to evaluate the change in means between data collected from Lake Carmi before aeration to data collected during this study. A threshold of $\alpha = 0.05$ was used to determine significant difference. R statistical software was used to process the raw data collected from the profiling system and meteorological station. The rLakeAnalyzer package was used to estimate lake bathymetry, process time series data into heat plots of temperature and DO, and to calculate Schmidt stability of the water column from vertical temperature measurements (Read et al., 2011). ODR was calculated as the change in hypolimnetic DO measured by the deepest sensor in each lake at the onset of stratification until DO was depleted or remixing occurred. The rate was calculated as the difference between DO concentration divided by the time between the two measurements (Burns, 1995; Lemmin, 2020; Rhodes et al., 2017).

The mapping software ArcGIS Pro was used to interpolate the sediment bulk density and the concentration of P and metals in Missisquoi Bay in between sampling sites. Spatially autocorrelated data can be modeled with a semivariogram which plots average dissimilarity of paired points against separation distance between those points. The semivariogram was then used as the underlying model to create a prediction surface (kriging) by taking a weighted average of known points (Isaaks & Srivastava, 1989; Olea, 2006).

Kriging methods have been used in previous studies to estimate sediment phosphorus concentrations (John et al., 2021; Puttonen et al., 2014). Empirical Bayesian Kriging (EBK) was chosen as the interpolation method for this study because parameters are assigned through a process of multiple simulations on data subsets to minimize error. New values are estimated successively at each input location and a new semivariogram is estimated from each set of simulated data. This process is repeated to obtain an average semivariogram from multiple results. EBK has been shown to model complex environmental data sets better than other kriging methods because it includes the uncertainty of the underlying semivariogram and can account for moderately nonstationary data (Krivoruchko & Gribov, 2019; Samsonova et al., 2017).

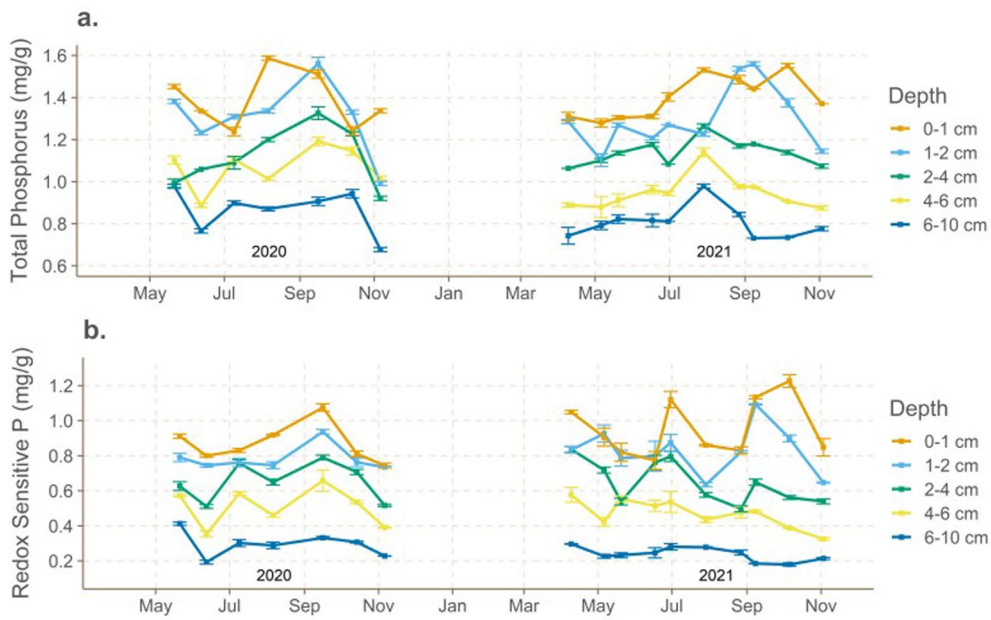

Figure 2. Lake Carmi 2020 and 2021 sediment data time series of (a) total phosphorus (TP) extracted by Aqua Regia digestion and (b) redox sensitive P obtained by ascorbate extraction per gram of dried sediment at each respective depth. Error bars represent the standard error of triplicate extractions.

Measured point values were mapped in ArcGIS Pro, and EBK analysis was run in the geostatistical analysis package for each sediment depth fraction. Prediction surface results were cross validated by successively excluding experimental points and comparing the known value with the interpolated value at that location. Results were generalized by calculating the root mean square error (RMSE) of interpolation:

$$\mathrm{RMSE} = \sqrt{\frac{\sum_{i=1}^{n}(\hat{z}(s_i) - z(s_i))^2}{n}} \tag{1}$$

where $\hat{z}(s_i)$ is the interpolated value, $z(s_i)$ is the measured value at point s_i, and n is the number of data points. The subscript i denotes the corresponding individual values of the paired measured and interpolated component.

The resulting estimation raster was clipped by the Missisquoi Bay border shapefile and binned to estimate the total area for each range of values. Sediment bulk density and P mass were also interpolated in this way. The resulting layers were further clipped by depth to remove shallow areas that are not predicted to experience low DO or contribute significantly to internal P loading.

3. Results

3.1. Sediment and Water Geochemistry

3.1.1. Lake Carmi

Sediment cores were collected from Lake Carmi in 2020 and 2021 during both mixed and stratified conditions at the sampling site (Figure 2). These samples had a mean TP concentration of 1.03 mg/g of dry sediment (range: 0.89–1.17 mg/g). On average, redox sensitive P concentrations were 49.3% (0.50 mg/g) of TP in the top 10 cm. Redox sensitive P ranged from 0.40 to 0.62 mg/g. The top centimeter of sediment had an average concentration of 0.92 mg/g redox sensitive P and 1.39 mg/g TP. The concentration of TP and the proportion of redox sensitive P generally decreased with depth. This upper layer had the greatest change in concentration. The top 10 cm of sediment had an average dry sediment bulk density of 0.10 g/cm^3 which results in an average redox sensitive P mass of 5.15 g/m^2. There was a mean Fe:P of 20.3 by mass (Figure S2 in Supporting Information S1), and a positive correlation between TP and total Fe ($r = 0.77$, $n = 17$, $p < 0.0001$) and between redox sensitive P and Fe ($r = 0.63$, $n = 17$, $p < 0.0001$).

Figure 3. Lake Carmi water column samples by VT DEC showing (a) water column total phosphorus (TP) with the 22 µg/L total maximum daily load (TMDL) target shown as a dashed line, (b) surface and bottom Fe, and (c) surface and bottom Mn, all on a log10 scale. Aeration began in 2019. Fe and Mn data are not available before 2018 (gray shaded area).

Total P in the water column exceeded the TMDL target of 22 µg/L during each study year (Figure 4a). The concentration of TP in spring sampling by the VT DEC was 18.4 µg/L ± 0.9 (SE). High TP in the bottom water relative to the rest of the water column (2–9 times higher TP) was observed in July and August at the deepest monitoring station under stratified conditions. Reducible metals also increased in the bottom water during this time (Figures 3b and 3c). Concentrations of Mn and Fe in July 2018 were 40–50 times higher than in the spring or fall. There was a positive correlation between bottom water TP and both total dissolved Fe ($r = 0.94$, $n = 89$, $p < 0.0001$) and Mn ($r = 0.80$, $n = 89$, $p < 0.0001$). Surface TP increased through the summer following mixing of the water column and averaged 49.7 µg/L ± 2.2 (SE) after fall turnover, well above the 22 µg/L TMDL target. The highest surface concentrations were recorded on 28 August 2017 (94 µg/L TP), 14 October 2020 (81 µg/L TP) and 29 August 2022 (83 µg/L TP).

3.1.2. Missisquoi Bay

Sediment bound P varied spatially across Missisquoi Bay. The mean TP in the top 10 cm across all sites was 1.00 mg/g of dry sediment (range: 0.63–1.42 mg/g). Redox sensitive P varied in concentration from 0.13 to 0.70 mg/g and was 38% of TP on average. Spatial interpolation shows that the highest concentrations were in the deeper waters of the western bay (north of the U.S.—Canada border), along the east of the bay, and near the southwestern outlet (Figure 4). Concentrations were lower in shallow areas such as the northwestern lobe, along the western shore, or the west side of the southeast lobe. The RMSE of interpolated P concentration was 0.10. Sediment samples from Missisquoi Bay had a mean Fe:P of 44.43 (range: 26.27–60.41) by mass (Figure S3 in Supporting Information S1). There was a positive correlation between TP and total Fe ($r = 0.92$, $n = 110$, $p < 0.0001$) and between redox sensitive P and Fe ($r = 0.88$, $n = 110$, $p < 0.0001$) across all sites.

The mass of available P depends on the bulk density of sediment which also varies spatially in Missisquoi Bay. Dry sediment bulk density ranged from 0.30 to 0.73 g/cm^3 with an interpolation RMSE of 0.07 (Figure 5a).

10.1029/2023WR034813

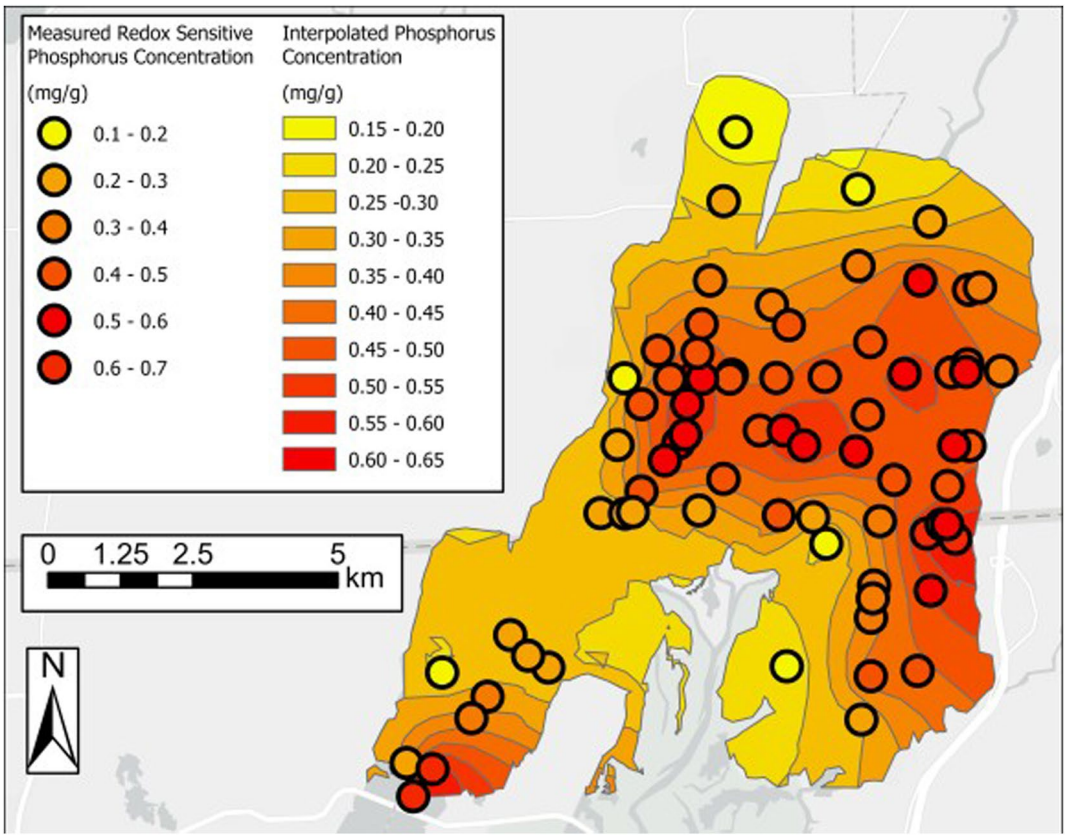

Figure 4. Measured redox sensitive P concentration in the upper 10 cm at sampling sites in Missisquoi Bay in Lake Champlain and the interpolated concentration surface. The gap in samples through the western channel is due to the presence of very coarse sediment that prevented core retrieval. See Figure 5b for depth contours.

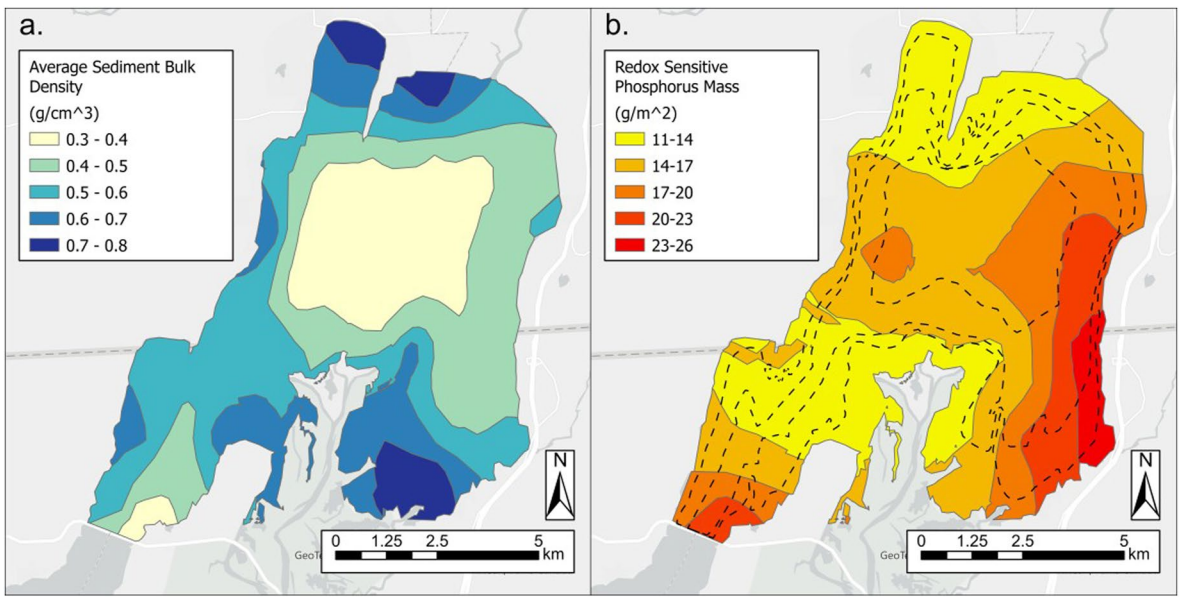

Figure 5. Interpolated surface of the upper 10 cm of sediment in Missisquoi Bay in Lake Champlain. (a) Average sediment bulk density and (b) total redox sensitive P mass in the upper 10 cm by area. Bathymetry contours are shown for reference as dashed black lines for depths of 2, 3, and 4 m.

10.1029/2023WR034813

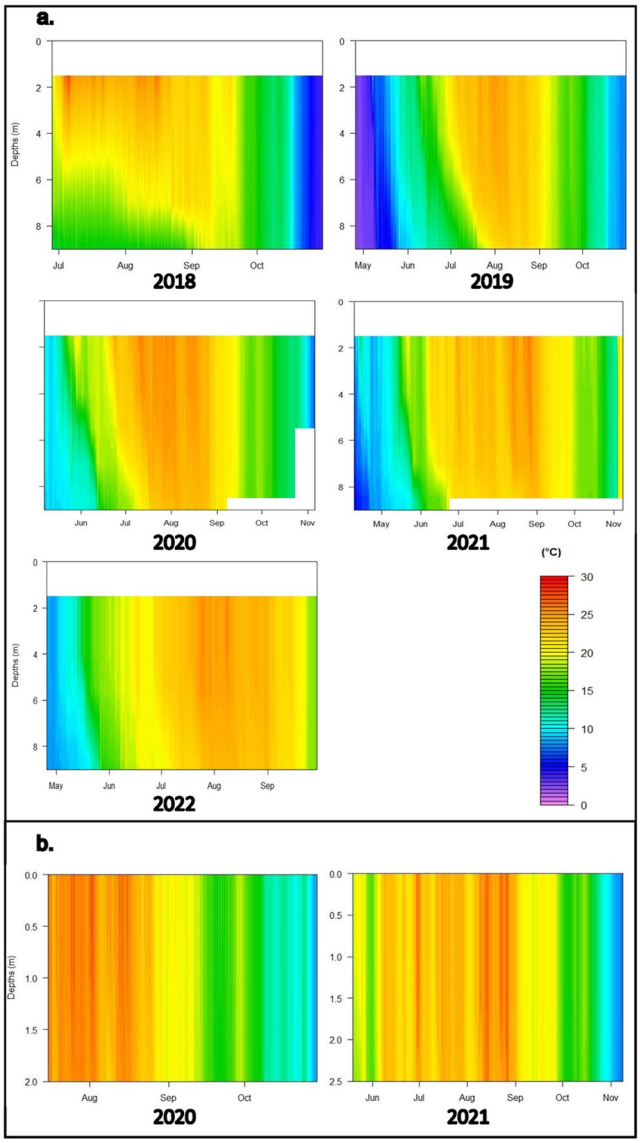

Figure 6. (a) Thermal profiles of Lake Carmi derived from fixed chain temperature sensors in 2018–2022. Aeration began in Lake Carmi in 2019. (b) Thermal profiles of Missisquoi Bay derived from Sonde profiler data in 2020 and 2021. Contour intervals at 0.5°C. White areas indicate no data due to sensor placement or failure.

Sediment density generally decreased toward the deeper central bay. Samples from shallow areas near shore had nearly twice the dry bulk density of those from the middle of the bay. The overlapping areas with high redox sensitive P concentration and high bulk density had the highest P mass. Redox sensitive P mass in the top 10 cm ranged from 10 g/m^2 in the northern bay to 31 g/m^2 in the east/southeast and near the outlet of the bay with an interpolation RMSE of 4.6 g/m^2 (Figure 5b). The total redox sensitive P mass in Missisquoi Bay was calculated from the range of interpolated values and the area of each zone (Table S1 in Supporting Information S1). We estimated that there is between 76,000 and 84,000 kg of redox sensitive P in the top cm of sediment, and as much as 1,398,000 kg in the top 10 cm. Estimates of P mass are lower if the area is constrained by depth (Figure 5b).

Surface water TP in Missisquoi Bay averaged around 48 μg/L between 2017 and 2020. Concentrations were typically elevated in the spring, and then dropped to 20–40 μg/L in May and June. TP increased in the summer and peaked in late August through early October (60–90 μg/L). TP was often nearly the same between the two LTMP monitoring stations in Missisquoi Bay, but sometimes varied by 10–20 μg/L on the same sampling day. The largest difference between the two sites was 23.4 μg/L on 9/03/21. Elevated P, Mn, and Fe were observed in the bottom water during anoxic events. Concentrations of Mn were up to 25 times higher at sites with low bottom DO compared sites with fully mixed conditions. TP was correlated both with both Fe ($r = 0.84$, $n = 84$, $p < 0.0001$) and Mn ($r = 0.83$, $n = 84$, $p < 0.0001$) in bottom water through this sampling.

3.2. Water Column Dynamics

3.2.1. Lake Carmi

Lake Carmi is a dimictic lake that, in the absence of aeration, fully mixes in the spring and fall, and thermally stratifies in winter and summer (Figure 6a). In 2018, Lake Carmi was stratified when sensors were deployed. VT DEC sampling shows a well-mixed water column on 14 May and stratified conditions at their next sampling date on 31 May. It remained stratified until turnover in mid-September. The water column partially mixed down to 6 m in July and August, and down to 7 m in late August. The maximum bottom water temperature in 2018 was 22.85°C and occurred during fall turnover. The average difference in surface and bottom temperature was 4.50°C with a maximum difference of 11.50°C on 5 July. Bi-weekly sampling by VT DEC shows full mixing by mid to late September in 2016 and 2017 as well.

The aeration system was installed in 2019 and turned on after stratification had already developed. It was turned on in years 2020–2022 at the onset of stratification and once bottom water temperature reached 4°C. There was downtime (parts failure, maintenance, overheating) of one or both compressors in 2019, 2020, and 2021. In 2022, the aeration system remained functional for the entire season. This made full analysis of the system performance difficult, but there were significant changes in the lake due to partial aeration. Mean summer bottom water temperature increased by 3.5°C ($p < 0.0001$) and water column stability was decreased by 75% ($p < 0.0001$) (Table 1). The water column was less stable during periods of active aeration (Figure 7). In 2018, Lake Carmi had a maximum and average Schmidt stability of 87 and 26.6 J/m^2 respectively. Aeration lowered the maximum Schmidt stability of Lake Carmi slightly, and the average stability was reduced by two thirds over the entire monitoring period (Table S2 in Supporting Information S1).

Aeration changed the mixing regime of Lake Carmi from dimictic to polymictic. The thermal profile shows stratified water temperature in 2018 until mid-September (Figure 6a). During aerated years, nearly uniform temperatures were observed multiple times in July and August, indicating mixing of the water column periodically

Table 1
July Through September Mean Values of Water Quality Metrics for Lake Carmi

	Pre-aeration summer mean (2016–2018)	Aerated summer mean (2019–2022)	*t*-test *p*-value
Bottom DO (mg/L)	0.77	3.96	<0.0001
Bottom Temp (°C)	18.30	21.81	<0.0001
Schmidt Stability (J/m^2)	40.09	9.37	<0.0001
Surface TP (μg/L)	37.09	47.00	0.0204
Bottom TP (μg/L)	71.86	47.12	0.0454
Bottom Fe (μg/L)	569.64	99.34	0.0005
Bottom Mn (μg/L)	787.44	113.34	<0.0001

Note. Data was collected by the Vermont Department of Environmental Conservation pre-aeration (n = 22) and during four aerated years (n = 37). *T*-test values represent the comparison of mean values between these two periods.

through the summer. There was a slow breakdown in stratification once the aerators were turned on that resulted in more frequent, although not continuous, mixing over the summer. The maximum water temperature difference between surface and bottom water was smaller for each aerated season and occurred before aeration began instead of mid-summer. The average temperature difference was 2–4 times smaller between 15 June and 15 September. Average bottom water temperature increased from around 17.6°C in 2018 before fall turnover to 22.0°C in 2020 and 22.2°C in 2021 over the same period. Continuous mixing was not achieved in any of the study years, but there was a shift to a polymictic mixing regime with shorter periods of weaker stratification compared to the pre-aeration dimictic system.

The decrease in water column stability made Lake Carmi more prone to wind-driven mixing throughout the summer and fall. Between 2020 and 2022 there were 96 wind events that resulted in partial mixing (defined as a 50% reduction in water column stability), and 38 events that resulted in full mixing of the water column following stratification (Figure S4 in Supporting Information S1). About 85% of those events were during aeration. Of the mixing events when aeration was off, all but one partial mixing event (25 June 2021, windspeed 5.5 m/s) occurred in the early spring or late fall when water column stability is naturally low. Windspeed was not measured in 2018, however water column stability data show that there were 11 partial mixing events, all after 8 September. There were three full mixing events after 21 September 2018. There were no partial or full mixing events during the summer months in 2018 when internal P loading was observed.

3.2.2. Missisquoi Bay

Missisquoi Bay experienced brief periods of spatially heterogeneous stratification and anoxia mostly in August and September (Figure 6b). Bottom water temperature reached a maximum of 26.29–28.85°C over the study period. The average difference in surface and bottom temperature was 0.37°C with a maximum difference of 7.83°C. This small temperature difference and shallow depth results in a relatively unstable water column. In 2018–2021, Missisquoi Bay had a maximum and average Schmidt stability of 16 and 0.95 J/m^2 respectively (Table S2 in Supporting Information S1). During the study period in 2020 and 2021 there were over 1,000 partial mixing events and 606 full mixing events (Figure S5 in Supporting Information S1).

3.3. Dissolved Oxygen

3.3.1. Lake Carmi

DO responded to the shift in mixing dynamics. Mean summer bottom water DO increased by over 3.5 mg/L (p < 0.0001) (Table 1). In Lake Carmi there were over 92.6 cumulative days of bottom DO below 1 mg/L in 2018 before aeration (half meter above SWI). The hypolimnion was already anoxic at the time of sensor deployment and it remained so until turnover in September (Figure 8). VT DEC data show low DO at a depth of 8 m

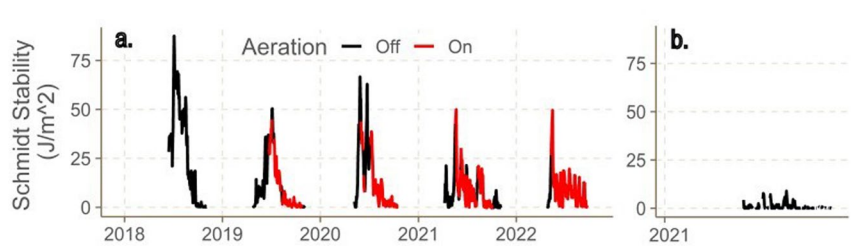

Figure 7. (a) Water column stability of Lake Carmi calculated as Schmidt stability (J/m^2). The stability during active aeration is plotted in red. The black line represents the natural system or periods when aeration was off. (b) Schmidt stability of Missisquoi Bay in 2021 included for comparison. Only 1 year is shown for Missisquoi Bay which had similar mean and maximum Schmidt stability during each study year.

10.1029/2023WR034813

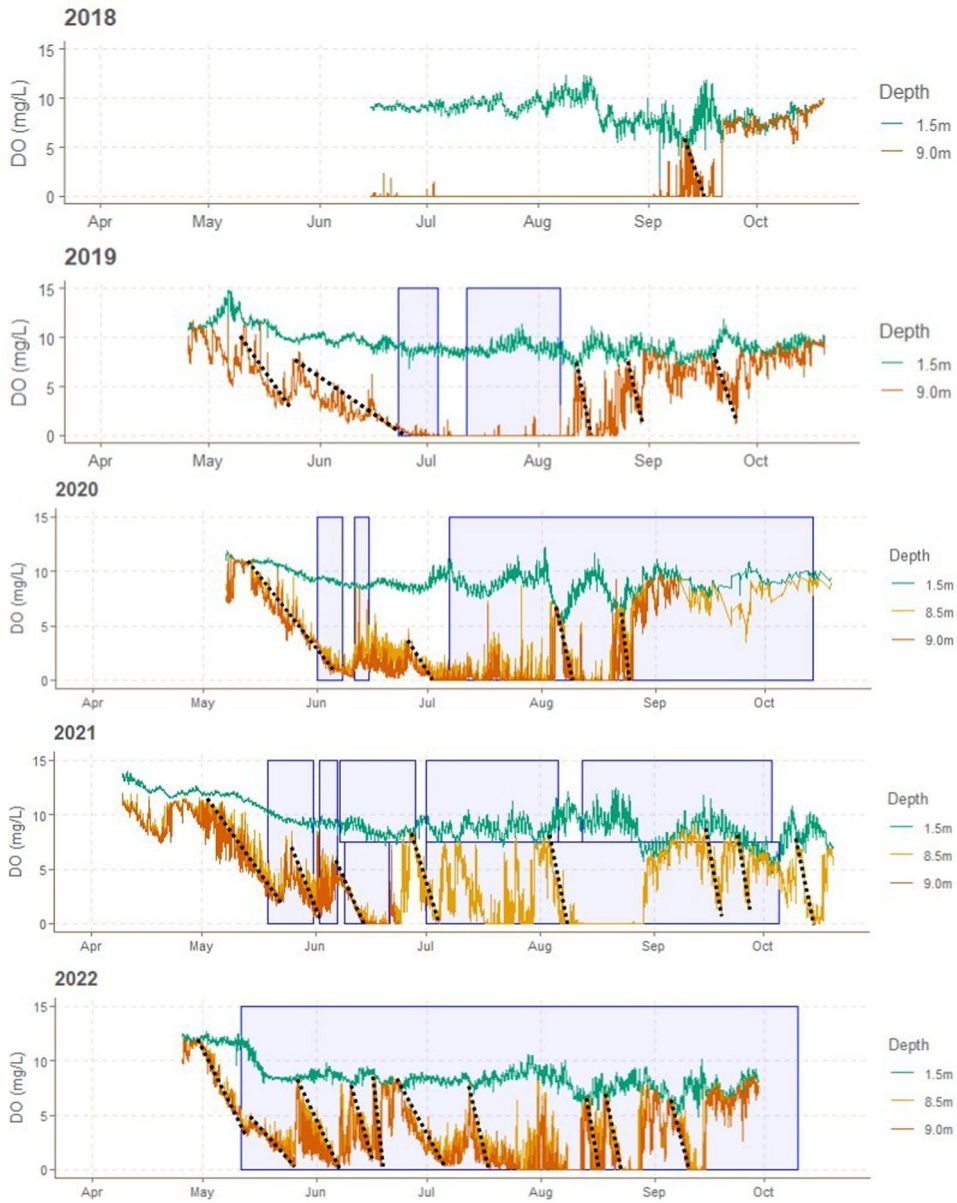

Figure 8. Lake Carmi surface and bottom dissolved oxygen (DO) recorded by fixed chain sensors. The blue shaded regions indicate aerator functionality. In 2021, aeration is broken up by the northern compressor array (top) and southern array (bottom). Example regression lines used to calculate hypolimnetic oxygen demand rates during periods of stratification are shown as black dashed lines.

(2.35 mg/L) under stratified conditions on 31 May 2018. In the years with aeration, average bottom DO was above the 2.5 mg/L target established by the VT DEC. Low bottom DO was more intermittent but did still persist for significant periods. There were 57, 57.7, and 46.5 cumulative days where bottom DO fell below 1 mg/L in 2019, 2020, and 2022 respectively. The bottom-most fixed sensor failed in 2021, but the duration of low DO was nearly the same at 1 m above the SWI compared to 2019 and 2020. The layer of anoxia was also generally shallower with aeration. It reached a depth of 6 m for several days in 2018. Anoxia only briefly reached a depth of 7 m in 2019 and 2020, and 7.5 m in 2021 and 2022.

ODR increased in Lake Carmi with aeration. The initial depletion of oxygen following spring mixing occurred over a period of over 1 month in 2018 and 2019 without aeration (mid-May to mid-June). Bottom DO depletion in spring of 2020–2022 occurred at a similar rate before the aerators were turned on. Aeration slowed the

10.1029/2023WR034813

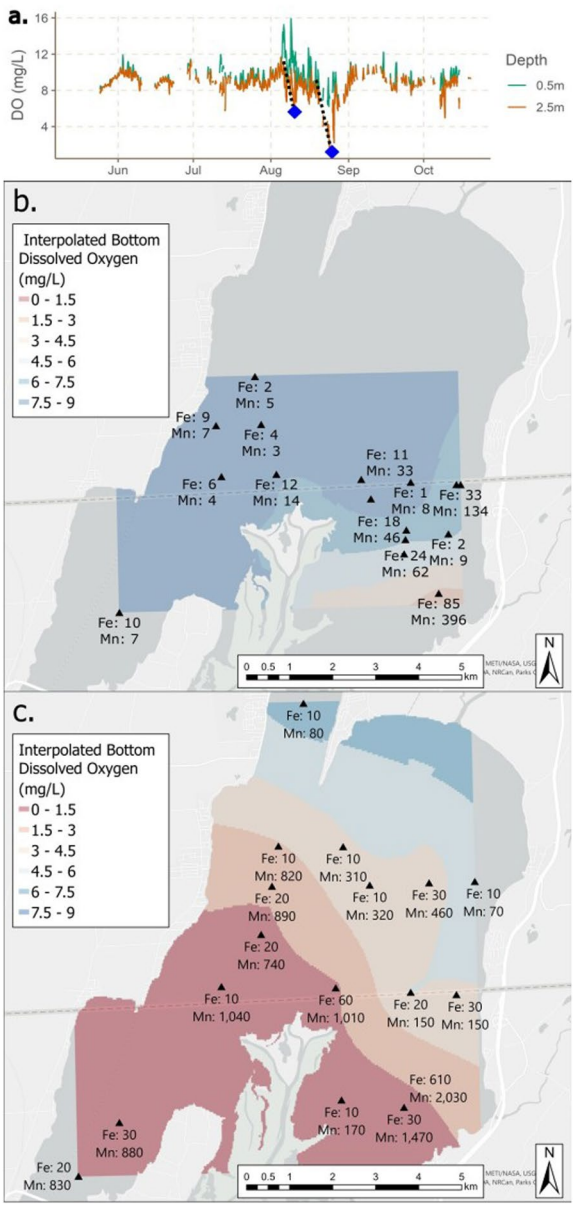

Figure 9. (a) 2021 time series of surface and bottom dissolved oxygen (DO) concentrations at the monitoring platform in Missisquoi Bay. Gaps in the data correspond to operational downtime of the profiler. Spatial interpolations of bottom DO along with bottom dissolved Fe and Mn concentrations (mg/L) are shown for the low oxygen events observed on (b) 10 August 2021 and (c) 25 August 2021. Example regression lines used to calculate hypolimnetic oxygen demand rates during periods of stratification are shown as black dashed lines.

rate by about two thirds (0.37 mg/L/day without aeration to 0.12 mg/L/day with aeration) before the hypolimnion became anoxic (Figure 8). Oxygen demand increased following subsequent mixing events that replenished bottom DO. This was seen once in 2018 at the start of fall turnover. A partial mixing of the water column was followed by rapid depletion of bottom DO (0.63 mg/L/day). This rate was exceeded each year with aeration. The highest ODR (1.3 mg/L/day) was observed in 2021 during a shutdown in aeration after bottom water temperatures had been raised above normal. The rate of oxygen depletion was not solely dependent on bottom water temperatures. In 2021, DO fell at a rate of 1.08 mg/L per day following subsequent mixing and a bottom water temperature of 17°C, the same temperature seen in June of that year when the depletion rate was only 0.37 mg/L per day.

3.3.2. Missisquoi Bay

Bottom water DO in Missisquoi Bay was very responsive to brief periods of stratification. The minimum bottom DO at the platform site ranged from 5.8 mg/L in 2020 to 0.24 mg/L in 2021 (Figure 9a). LTMP sampling shows similar results at their two monitoring locations in the bay. The hypolimnion at these sites sometimes had low DO (e.g., 2.17 mg/L at station 50 in 2017, 2.38 mg/L at station 53 in 2021) but was never fully anoxic. We sampled across areas of the bay on several days when conditions favored stratification. The most widespread low DO that we encountered was on 25 August 2021, the same day as the lowest platform reading (Figure 9c). Manual sonde readings of DO just above the SWI were below 1 mg/L in the southeast lobe of the bay. Bottom DO was also low (0.48–2.74 mg/L) in the southwest and western side. DO increased to the northeast (2.8–6.07 mg/L) and northwestern lobe (7.36 mg/L). Sampling on 10 August 2021 also captured a difference in bottom DO across the bay, but no anoxia (Figure 9b). Bottom DO south of the monitoring platform was 2.65 mg/L.

Moving north, bottom DO in the rest of the southeast lobe ranged from 5.63 to 6.96 mg/L. Other samples in the bay were even higher (7.52–9.77 mg/L). Oxygen demand was relatively high during the few periods of stratification over the monitoring period. In August and September 2020 bottom DO fell at a rate just over 0.5 mg/L/day on two occasions but remixing occurred before the hypolimnion went anoxic. In August 2021, ODR were 1.32 and 1.43 mg/L/day leading to two periods of low bottom DO.

3.4. Phosphorus Response to Dissolved Oxygen

3.4.1. Lake Carmi

During aeration, there was no significant difference in mean surface TP concentrations during spring through 15 July compared to pre-aeration concentration (20.7 ± 1.4 μg/L pre-aeration, 20.6 ± 0.8 μg/L post aeration, *t*-test: $p = 0.9718$). In years with aeration, mean surface TP in July through September increased from 37.9 to 47.0 μg/L (p value = 0.020) (Table 1). Over that same period, VT DEC data showed that mean bottom water TP decreased from 71.86 to 47.12 μg/L ($p = 0.045$). When compared with the daily bottom water samples collected in this study, there was no significant change in bottom TP (July–September mean value: 72.85 μg/L). Bottom water metals (Fe and Mn) concentrations were also significantly lower in the VT DEC samples during aeration ($p = 0.0005$, $p < 0.0001$). On concurrent sampling days, the TP concentration in bottom water collected by the ISCO were very similar to the bottom water samples collected by the VT DEC during mixed conditions (Figure 10). Platform ISCO samples were on average 1.7 times higher than samples collected by VT DEC at 8 m during stratified conditions.

Figure 10. Bottom and surface water total phosphorus (TP) collected in 2020/2021 from Lake Carmi. Orange segments represent periods of bottom water anoxia which end with mixing events that replenish dissolved oxygen to the water column. The red dashed line is the total maximum daily load target of 22 µg/L.

The daily ISCO sampling also captured internal loading events that were not observed in the VT DEC data set. Large increases in bottom TP were seen at the onset of anoxia. In 2020 the VT DEC sampling captured an increase in bottom TP during the first low bottom DO (<2.5 mg/L) before the ISCO was deployed. Additional increases in TP were captured in water sampled by the ISCO under low DO conditions. TP rose to 45 µg/L within 24 hr of DO falling below 1 mg/L for the first time, and then spiked to 311 µg/L when bottom DO was depleted. In 2021, bottom TP reached 294 µg/L 24 hr after DO fell below 1 mg/L for the first time, a 6× increase in concentration. Subsequent anoxic events following mixing events caused similar spikes in bottom TP within 24–48 hr (Figure 10).

Phosphorus in the rest of the water column increased over the summer during each study year. Large increases in surface TP were observed when periods of internal loading were followed by full or partial water column mixing. In 2018, surface TP increased by 29.5%–30.3 µg/L in July following increased bottom P and partial mixing to 6 m. TP increased by another 31% in August when mixing reached 7 m. The maximum surface TP of 43.1 µg/L was reached in mid-September after full mixing of the water column. This concentration was exceeded over a month earlier (late June to early August) in each study year with aeration. Alternating periods of anoxia and mixing in 2019–2022 resulted in elevated TP earlier in the summer and higher maximum concentrations (63.0, 81.5, 63.0, and 83.0 µg/L respectively) following full mixing.

The two other VT DEC sampling sites did not exhibit as high TP concentrations as the central monitoring site (Figure S5 in Supporting Information S1). The northern site (Site #3) did not have anoxic bottom water on any of the sampling days before or during aeration. The highest TP concentrations were both surface samples (69.0 and 79.9 µg/L) collected on 13 September 2017 and 27 August 2021. The southern site (Site #2) experienced some hypolimnetic anoxia pre-aeration, but none on sampling days during the aerated years. The largest difference between top and bottom TP (27.7 µg/L at the surface to 49.9 µg/L at 6 m) was sampled on 27 July 2017 when bottom DO was 0.2 mg/L. The highest TP (171 µg/L) was sampled at the surface on 13 September 2017 when bottom TP was below 40 µg/L. Fe and Mn were not tested at VT DEC site #3. At site #2, both Fe and Mn were elevated in bottom water samples relative to surface water at the onset of anoxia, but bottom TP was only slightly higher than surface concentrations.

3.4.2. Missisquoi Bay

Bottom water samples collected from sites with high sediment P mass during two low DO events in 2021 showed elevated concentrations of dissolved P and Mn. On 10 August 2021 when there was one site with low DO (2.65 mg/L), dissolved P was at a similar concentration to the rest of the bay, but dissolved Mn was 8× higher than nearby sites. On 25 August 2021, during sampling when much of the bay had low bottom DO, several sites had dissolved P over 60 µg/L with a maximum of 177 µg/L. Sites that were well mixed and oxygenated had an average dissolved P of 45 µg/L. Bottom water dissolved Mn was also elevated in areas with low DO (up to 20× higher than well mixed sites). Sites with lower P mass did not have as high of concentrations of bottom water dissolved P during this sampling.

4. Discussion

4.1. Overview

This research highlights the complexity of managing legacy P in shallow eutrophic systems. Lake Carmi and Missisquoi Bay both experience internal P loading coupled with redox driven Fe cycling at the SWI. This is illustrated by the ratios of those elements in their respective lake sediments (Figures S2 and S3 in Supporting Information S1). This is also supported by observed co-enrichment and positive correlation of bottom water in P, Mn, and Fe during periods and at locations where low oxygen conditions were detected at both sites (Figures 3 and 9). However, the temporal and spatial distribution of internal loading events differs between these two systems due to differences in hydrodynamics, which controls the development and persistence of stratification and a reducing SWI during summer months. In subsequent sections, we (a) discuss the drivers of internal loading of legacy P in both lake sites derived from robust spatial and temporal monitoring campaigns, (b) identify how internal loading and its drivers change in response to an aeration intervention as captured by high frequency and long-term time series, and (c) explore how these novel data and analyses can inform subsequent efforts to suppress internal loading in systems with similar characteristics. Our use of high-frequency data illustrates that this type of monitoring could also be proactively leveraged to inform intervention plans, and used to develop models that predict the impact of intervention scenarios before implementation.

4.2. Fe Mediated P Cycling and Seasonal Controls of Internal Loading in Shallow Dimictic Systems

High frequency in-situ monitoring confirmed the persistent stratification and low oxygen conditions at the SWI in the central trough of Lake Carmi as was also observed in the long-term VT DEC monitoring. There were no mixing events or substantial increases in bottom water DO observed between bi-weekly VT DEC sampling events in 2018 (Figure 8). There was a buildup of P and Fe in the hypolimnion during prolonged stratification due to internal loading associated with sustained anoxia at the SWI (Figure 3). These conditions were less severe at the shallower VT DEC monitoring sites, suggesting that internal loading is largely depth dependent in this relatively shallow dimictic system (Figure S5 in Supporting Information S1). Our data show that the deepest segments have low sensitivity to wind driven mixing outside of spring and fall turnover, suggesting a seasonal trigger of the release of legacy P to the photic zone in the pre-aeration system. This was observed in the delay between P in the hypolimnion and subsequent increase in surface concentration following the gradual deepening of the thermocline (Figure 6). Our analysis suggests that the deep central trough should be the focal point of intervention to suppress redox driven P release (Figure 1). Shallow dimictic systems like Lake Carmi that are resistant to summer wind driven mixing are likely to experience depth dependent internal loading associated with anoxia at the SWI.

4.3. Heterogeneous Legacy Phosphorus Distribution and Loading Dynamics in a Large Polymictic Bay

High frequency in-situ monitoring confirmed the highly transient nature of low level thermal stratification (often less than 1°C), and consequent low oxygen conditions at the SWI, and thus redox driven internal loading in Missisquoi Bay, which is consistent with our previous findings at this site (Giles et al., 2016; Isles et al., 2015; Smith et al., 2011). However, our spatial sampling campaigns revealed spatially heterogeneous internal P loading that was not captured by the monitoring platform or in our previous work. Bottom water P concentrations varied by a factor of 2–3 across the bay during the same day, and Mn by a factor of 10 across a very similar range of depths (2.3–4.4 m). This demonstrates that despite the nearly uniform depth of the bay and ubiquitously relatively high concentration of redox sensitive P in sediments (Figure 4), conditions that promote internal loading were spatially highly dynamic. This is due to the sensitivity of the bay's hydrodynamics to wind, which promotes variable redox conditions at the SWI. For example, on 25 August 2021 the entire southern half of the bay had low oxygen bottom water (0.26–2.74 mg/L DO), and relatively high bottom water P and Mn (51–171 μg/L TP, 0.17–1.47 mg/L Mn) (Figure 9). Furthermore, this was a condition that had lasted for a few days, indicating that this was a relatively large scale internal loading event, at least in the portion of the bay with the smallest fetch for a southwestern wind. Conversely, on 10 August 2021, low oxygen conditions (2.3 mg/L DO) and high bottom water Mn concentrations (0.39 mg/L) were only prevalent in the SE lobe of the bay, indicating that event was hyper-localized in the most sheltered portion of the bay, as wind forcing mixed the rest of the bay.

Wind data and frequency of turnover (Figure S4 in Supporting Information S1) suggest that there is a very subtle threshold for wind driven mixing to occur in Missisquoi Bay given its shallow depth and large surface area

compared to Lake Carmi. This is likely why we did not observe chemical evidence of internal loading events in the northern portion of the bay due to its large fetch under the predominant southwestern wind orientation of the summer, even under the relatively hot and calm conditions under which the 25 August 2021 sampling events occurred. Similarly, bottom water P and Mn concentrations were relatively low with little variation during fully mixed sampling events (Figure S6 in Supporting Information S1). As such, our analysis suggests that in systems like Missisquoi Bay (high surface area, high sediment surface area to volume ratio, similar shallow depth), small differences in physical characteristics and hydrodynamic response of different regions to the prevailing summer wind direction can control the extent to which any given region of the lake may contribute to internal loading P budgets. The relative contribution of these regions to internal loading will vary as wind driven forcing of hydrodynamics changes in response to the weather. Because of this, wind driven forcing is critical to consider with targeted treatment plans of shallow polymictic systems.

4.4. Aeration's Impact on Internal P Loading in Lake Carmi

Aeration caused a dramatic change in mixing regime and in the thickness and duration of low oxygen conditions in Lake Carmi. We observed a significant decrease in water column stability when the aerator was functioning (Table 1, Figure 7), leading to increased wind sensitivity and mixing that affected the deepest lake segments (Figure S4 in Supporting Information S1, Figure 6). However, aeration did not prevent periods of anoxia even when fully functional leading to sharp increases in bottom water P, even with only transient minor stratification (Figure 10). An increase in ODR from aeration and water column mixing has been observed in previous research due to turbulence at the SWI and an increase in diffusive gradient (Beutel & Horne, 1999; Bierlein et al., 2017; Bryant et al., 2010). It is also likely that higher bottom water temperatures led to increased rates of organic matter remineralization and oxygen consumption (Bergstrom et al., 2010; Niemisto et al., 2016; Rosa & Burns, 1987; Sobek et al., 2017).

Contrary to our predictions, aeration resulted in cycling between weakly stratified conditions that promote internal loading and full wind driven summer water column mixing, leading to an earlier increase in surface TP and higher average summer TP relative to pre-aeration years (Table 1). Even with a fully functional aeration system in 2022, this wind driven dynamic between these two states persisted. The change in the temporal distribution of internal loading and subsequent mixing events that raise surface water TP is particularly striking in the context of the seasonal variability of TP in the water column between the pre-aeration and post-aeration VT DEC time series (Figure 3). The seasonal evolution of TP concentrations in post aeration VT DEC data sets are quite similar with a gradual buildup of the entire water column's TP concentrations after the aerator was turned on and these cycles between weekly stratified and fully mixed water column progress over the course of any given summer, whether the aerator was fully (2022) or partially (2019–2021) functional. The cycle between conditions that favor internal loading and water column mixing also explains the decrease in summer bottom TP and increase in surface TP as observed in the VT DEC data set (Table 1). This could also explain the observed decrease in mean Fe and Mn concentrations in the bottom water.

There was less of a buildup of benthic legacy P in bottom water throughout the summer and fall during aeration because it was brought to the surface earlier in more frequent intermittent pulses. This led to a higher concentration of surface TP earlier in the summer. Several of these pulses were captured by our daily sampling but missed by the less frequent VT DEC sampling (Table 1, Figure 10). This dynamic represents a shift from the large seasonal pulse of bottom water-accumulated P during fall turnover to one driven by episodic pulses of legacy P from summer wind mixing. Contrary to our initial hypothesis, post-aeration legacy sediment P behavior remained tightly coupled with Fe redox cycling, but our unique data set captures the shift in environmental drivers of the mobility of P in the water column. This shift was triggered by wind driven mixing in an aerated unstable and highly dynamic water column relative to its pre-aeration summer state. This result highlights a potential drawback of aeration. Not only is the system failing to adequately maintain DO at a concentration that prevents internal P loading, but the decreased water column stability results in more frequent mixing that transports reactive P to the photic zone.

4.5. Comparing Internal P Loading Dynamics and Drivers Between a Naturally Polymictic Bay and a Transformed Polymictic Lake

Lake Carmi and Missisquoi Bay both exhibit high concentrations of legacy P that contribute to internal loading associated with reducing conditions at the SWI. Before aeration, there was a distinct difference in the temporal

and spatial availability of legacy P in each system. In Lake Carmi, there was an increase in bottom water TP primarily in the deep central trough that was subsequently mixed into surface waters as the thermocline gradually deepened. In contrast, Missisquoi Bay was shown to have a heterogeneous release of legacy P during brief periods of stratification throughout the summer that was quickly mixed throughout the water column. Subtle changes in windspeed and direction appear to be an important driver of internal loading in Missisquoi Bay compared to Lake Carmi where more significant wind is required to mix the water column. Aeration altered the internal P loading dynamics and drivers in previously dimictic Lake Carmi to match more closely those in Missisquoi Bay, a polymictic system. During this study, both systems responded rapidly to low windspeed which resulted in transient stratification and a subsequent drop in bottom DO. The increased ODR in years with aeration that we observed in Lake Carmi nearly matched the ODR in Missisquoi Bay and were more than double the highest rate observed in 2018 before aeration (Figure 8). Aeration reproduced some of the environmental drivers of oxygen demand seen in Missisquoi Bay by significantly warming bottom water (Table 1) and likely increasing turbulence at the SWI. In both systems, we detected an increase in bottom water TP due to internal loading within 24–48 hr of anoxia. This timing aligns with observations in previous research in dimictic systems (Anderson et al., 2021; Wilkes, 2019).

We observed a similar increase of TP when bottom water went anoxic following reoxygenation throughout the season (Figure 10), showing that this timing appears to hold for subsequent cycles in polymictic systems. There is evidence from laboratory experiments that increasingly high concentrations of P are released from sediments from oscillating redox conditions compared to sustained reducing conditions (Wilkes, 2019). While bottom water DO controls legacy P release, the upward flux of legacy P to surface water is controlled largely by wind-induced by mixing events. Aeration increased the frequency of such events in Lake Carmi, and we observed a steady increase in surface TP during aeration caused by pulses of internal P throughout the summer followed by mixing of P-enriched bottom water. These P dynamics closely match those observed in Missisquoi Bay, a naturally polymictic system (Giles et al., 2016; Isles et al., 2015; Smith et al., 2011).

4.6. Implications for Managing Internal Loading of Legacy Phosphorus

Both Lake Carmi and Missisquoi Bay present challenges to mitigating internal P loading. External nutrient loads are still relatively high in both watersheds even though there has been progress in limiting P inputs (IJC, 2019; Laitta et al., 2020; Porterfield & Roy, 2021). In-lake efforts to suppress internal P loading are temporary management solutions if high external loads continue to contribute to cyanobacteria blooms and replenish legacy P pools (Carpenter et al., 2018; Paerl, 2014). High frequency data collected in Lake Carmi demonstrates how quickly anoxia can set up when bottom water is warm under very low level stratification. Even when aeration was active, it could take less than 5 days for anoxia to develop with less than 1°C temperature difference as observed in August 2020–2022 (Figure 8). Previous research shows that it takes approximately 5 days to replenish oxygen at the SWI once a bubble plume diffuser is activated in anoxic conditions (Bryant et al., 2011). We observed that even under continuous aeration, hypolimnetic anoxia persisted at the monitoring site until the water column mixed. Lake Carmi mixed more frequently due to aeration and the decrease in water column stability which unintentionally promoted internal loads of legacy P reaching the photic zone earlier in the season. By setting up an aeration system that only partially destabilizes the water column, the timing of internal loading is much less predictable and subject to subtle changes in the wind.

In Missisquoi Bay, we illustrate the challenges imposed by scale and wind-driven forcing of internal loading, where focused treatment of a smaller area would not be feasible given the potential for different portions of the large bay to contribute to internal loading depending on wind speeds and orientation. Internal P loading was observed to sometimes occur locally, but also nearly bay-wide during long periods of sustained low winds. Wind impacts on the extent and location of internal P loading in low water column stability systems provide a unique challenge and understudied consideration when assessing opportunities to suppress internal loading of legacy P.

5. Conclusions

This research highlights the challenges in managing internal P loading in shallow lake systems. Understanding the unique physical and geochemical drivers within each lake is critical to achieving water quality goals. Despite both Missisquoi Bay and Lake Carmi exhibiting P mobility coupled with Fe redox reactions, we observed distinct

differences in the drivers of internal P loading between the two systems. Differences in hydrodynamics resulted in different temporal and spatial legacy P availability. The use of high-frequency, real time monitoring in this study was critical in further defining the drivers of internal P loading in each system. We captured changes in P mobility over short time scales in response to aeration and changes in wind. These high-frequency time series can be a powerful tool to assess internal loading suppression methods by capturing physical and biogeochemical responses within each lake. Further research on how these responses vary spatially can be used to define target treatment areas, allowing for additional management options in systems like Missisquoi Bay where there is a size limitation for many interventions. Our research illustrates the complexities and challenges associated with managing internal loading, but also clearly highlights the power of increasingly available high-frequency sensor data that can be used to better understand the impacts of interventions in real-time and adjust management strategies.

Conflict of Interest

The authors declare no conflicts of interest relevant to this study.

Data Availability Statement

The data collected as part of this research are publicly available at the Hydroshare repository (Kirol, 2023). Time series data were analyzed using R version 4.2.2 (R Core Team, 2021). R packages rLakeAnalyzer and ggplot2 were used to analyze water column data and create plots (Wickham, 2016; Winslow et al., 2019). Spatial data were analyzed using ESRI ArcGIS Pro version 3.0.0 (ESRI, 2022).

Acknowledgments

This study was partially funded by the Vermont Department of Environmental Conservation Grant 2020-CWF-Carmi-MON-01-A1, the United States Environmental Protection Agency under assistance agreement (LC00A00605) to NEIWPCC in partnership with the Lake Champlain Basin Program, the Vermont Water Center via the U.S. Geological Survey under Grant G21AP10630, and the National Science Foundation under VT EPSCoR Grant NSF OIA-1556770. Any opinions, findings, and conclusions or recommendations expressed in this material are those of the authors and do not necessarily reflect the views of any of the funding agencies. The authors would like to thank Saul Blocher, Austin Wilkes, and Pete Stangel for their help with sample collection, processing, and equipment maintenance, as well as Nicolas Perdrial for his valuable review of this research.

References

Anderson, H. S., Johengen, T. H., Godwin, C. M., Purcell, H., Alsip, P. J., Ruberg, S. A., & Mason, L. A. (2021). Continuous in situ nutrient analyzers pinpoint the onset and rate of internal P loading under anoxia in Lake Erie's central basin. *ACS ES&T Water*, *1*(4), 774–781. https://doi.org/10.1021/acsestwater.0c00138

Anschutz, P., Zhong, S., Sundby, B., Mucci, A., & Gobeil, C. (1998). Burial efficiency of phosphorus and the geochemistry of iron in continental margin sediments. *Limnology & Oceanography*, *43*(1), 53–64. https://doi.org/10.4319/lo.1998.43.1.0053

Bergstrom, I., Kortelainen, P., Sarvala, J., & Salonen, K. (2010). Effects of temperature and sediment properties on benthic CO_2 production in an oligotrophic boreal lake. *Freshwater Biology*, *55*(8), 1747–1757. https://doi.org/10.1111/j.1365-2427.2010.02408.x

Beutel, M. W., Hannoun, I., Pasek, J., & Bowman Kavanagh, K. (2007). Evaluation of hypolimnetic oxygen demand in a large eutrophic raw water reservoir, San Vicente Reservoir, Calif. *Journal of Environmental Engineering*, *133*(2), 130–138. https://doi.org/10.1061/(asce)0733-9372(2007)133:2(130)

Beutel, M. W., & Horne, A. J. (1999). A review of the effects of hypolimnetic oxygenation on lake and reservoir water quality. *Lake and Reservoir Management*, *15*(4), 285–297. https://doi.org/10.1080/07438149909354124

Bierlein, K. A., Rezvani, M., Socolofsky, S. A., Bryant, L. D., Wüest, A., & Little, J. C. (2017). Increased sediment oxygen flux in lakes and reservoirs: The impact of hypolimnetic oxygenation. *Water Resources Research*, *53*(6), 4876–4890. https://doi.org/10.1002/2016WR019850

Birk, S., Chapman, D., Carvalho, L., Spears, B. M., Andersen, H. E., Argillier, C., et al. (2020). Impacts of multiple stressors on freshwater biota across spatial scales and ecosystems. *Nature Ecology & Evolution*, *4*(8), 1060–1068. https://doi.org/10.1038/s41559-020-1216-4

Bormans, M., Maršálek, B., & Jančula, D. (2016). Controlling internal phosphorus loading in lakes by physical methods to reduce cyanobacterial blooms: A review. *Aquatic Ecology*, *50*(3), 407–422. https://doi.org/10.1007/s10452-015-9564-x

Boström, B., Andersen, J. M., Fleischer, S., & Jansson, M. (1988). Exchange of phosphorus across the sediment-water interface. In *Phosphorus in freshwater ecosystems* (pp. 229–244). Springer Netherlands. https://doi.org/10.1007/978-94-009-3109-1_14

Bowman, G. T., & Delfino, J. J. (1980). Sediment oxygen demand techniques: A review and comparison of laboratory and in situ systems. *Water Research*, *14*(5), 491–499. https://doi.org/10.1016/0043-1354(80)90215-8

Bryant, L. D., Gantzer, P. A., & Little, J. C. (2011). Increased sediment oxygen uptake caused by oxygenation-induced hypolimnetic mixing. *Water Research*, *45*(12), 3692–3703. https://doi.org/10.1016/j.watres.2011.04.018

Bryant, L. D., Lorrai, C., McGinnis, D. F., Brand, A., est, A. W., & Little, J. C. (2010). Variable sediment oxygen uptake in response to dynamic forcing. *Limnology & Oceanography*, *55*(2), 950–964. https://doi.org/10.4319/lo.2010.55.2.0950

Burns, N. M. (1995). Using hypolimnetic dissolved oxygen depletion rates for monitoring lakes. *New Zealand Journal of Marine & Freshwater Research*, *29*, 1–11. https://doi.org/10.1080/00288330.1995.9516634

Carey, C. C., Weathers, K. C., & Cottingham, K. L. (2009). Increases in phosphorus at the sediment-water interface may influence the initiation of cyanobacterial blooms in an oligotrophic lake. *SIL Proceedings, 1922–2010*, *30*(8), 1185–1188. https://doi.org/10.1080/03680770.2009.11923908

Carpenter, S. R., Booth, E. G., & Kucharik, C. J. (2018). Extreme precipitation and phosphorus loads from two agricultural watersheds. *Limnology & Oceanography*, *63*(3), 1221–1233. https://doi.org/10.1002/lno.10767

Castelletti, A., Pianosi, F., Soncini-Sessa, R., & Antenucci, J. P. (2010). A multiobjective response surface approach for improved water quality planning in lakes and reservoirs. *Water Resources Research*, *46*(6), W06502. https://doi.org/10.1029/2009WR008389

Cooke, G. D., Welch, E. B., Peterson, S., & Nichols, S. A. (2016). *Restoration and management of lakes and reservoirs*. CRC Press. https://doi.org/10.1201/9781420032109

Cottingham, K. L., Ewing, H. A., Greer, M. L., Carey, C. C., & Weathers, K. C. (2015). Cyanobacteria as biological drivers of lake nitrogen and phosphorus cycling. *Ecosphere*, *6*, 1–19. https://doi.org/10.1890/ES14-00174.1

Cowan, J. L. W., & Boynton, W. R. (1996). Sediment-water oxygen and nutrient exchanges along the longitudinal axis of Chesapeake Bay: Seasonal patterns, controlling factors and ecological significance. *Estuaries*, *19*(3), 562–580. https://doi.org/10.2307/1352518

Dadey, K. A., Janecek, T., & Klaus, A. (1992). Dry-bulk density: Its use and determination. In *Proceedings of the Ocean Drilling Program, 126 scientific results, Ocean Drilling Program*. https://doi.org/10.2973/odp.proc.sr.126.157.1992

ESRI. (2022). *ArcGIS Pro (version3.0.0)*. Esri Inc. Retrieved from https://www.esri.com/en-us/arcgis/products/arcgis-pro/overview

Franklin Watershed Committee. (2019). Aeration and Lake Carmi. Retrieved from https://www.franklinwatershed.org/uploads/1/0/6/3/106302261/aeration_and_lake_carmi.pdf

Giles, C. D., Isles, P. D. F., Manley, T., Xu, Y., Druschel, G. K., & Schroth, A. W. (2016). The mobility of phosphorus, iron, and manganese through the sediment–water continuum of a shallow eutrophic freshwater lake under stratified and mixed water-column conditions. *Biogeochemistry*, *127*(1), 15–34. https://doi.org/10.1007/s10533-015-0144-x

Giles, C. D., Lee, L. G., Cade-Menun, B. J., Hill, J. E., Isles, P. D. F., Schroth, A. W., & Druschel, G. K. (2015). Characterization of organic phosphorus form and bioavailability in lake sediments using 31 P nuclear magnetic resonance and enzymatic hydrolysis. *Journal of Environmental Quality*, *44*(3), 882–894. https://doi.org/10.2134/jeq2014.06.0273

Glibert, P. M. (2020). Harmful algae at the complex nexus of eutrophication and climate change. *Harmful Algae*, *91*, 101583. https://doi.org/10.1016/j.hal.2019.03.001

Håkanson, L. (2004). Internal loading: A new solution to an old problem in aquatic sciences. *Lakes & Reservoirs: Science, Policy and Management for Sustainable Use*, *9*(1), 3–23. https://doi.org/10.1111/j.1440-1770.2004.00230.x

Heisler, J., Glibert, P., Burkholder, J., Anderson, D., Cochlan, W., Dennison, W., et al. (2008). Eutrophication and harmful algal blooms: A scientific consensus. *Harmful Algae*, *8*(1), 3–13. https://doi.org/10.1016/j.hal.2008.08.006

Idso, S. B. (1973). On the concept of lake stability. *Limnology & Oceanography*, *18*(4), 681–683. https://doi.org/10.4319/lo.1973.18.4.0681

IJC. (2019). Nutrient loading and impacts in Lake Champlain, Missisquoi Bay, and the Richelieu River.

Isaaks, E. H., & Srivastava, M. R. (1989). *Applied geostatistics* (pp. 1–582). Oxford University Press.

Isles, P. D. F., Giles, C. D., Gearhart, T. A., Xu, Y., Druschel, G. K., & Schroth, A. W. (2015). Dynamic internal drivers of a historically severe cyanobacteria bloom in Lake Champlain revealed through comprehensive monitoring. *Journal of Great Lakes Research*, *41*(3), 818–829. https://doi.org/10.1016/j.jglr.2015.06.006

James, W. F. (2017). Internal phosphorus loading contributions from deposited and resuspended sediment to the Lake of the Woods. *Lake and Reservoir Management*, *33*(4), 347–359. https://doi.org/10.1080/10402381.2017.1312647

Jeppesen, E., Søndergaard, M., Jensen, J. P., Havens, K. E., Anneville, O., Carvalho, L., et al. (2005). Lake responses to reduced nutrient loading - An analysis of contemporary long-term data from 35 case studies. *Freshwater Biology*, *50*(10), 1747–1771. https://doi.org/10.1111/j.1365-2427.2005.01415.x

Jilbert, T., Couture, R. M., Huser, B. J., & Salonen, K. (2020). Preface: Restoration of eutrophic lakes: Current practices and future challenges. *Hydrobiologia*, *847*(21), 4343–4357. https://doi.org/10.1007/s10750-020-04457-x

John, K., Afu, S. M., Isong, I. A., Aki, E. E., Kebonye, N. M., Ayito, E. O., et al. (2021). Mapping soil properties with soil-environmental covariates using geostatistics and multivariate statistics. *International Journal of Environmental Science and Technology*, *18*(11), 3327–3342. https://doi.org/10.1007/s13762-020-03089-x

Katsev, S., Tsandev, I., L'Heureux, I., & Rancourt, D. G. (2006). Factors controlling long-term phosphorus efflux from lake sediments: Exploratory reactive-transport modeling. *Chemical Geology*, *234*(1–2), 127–147. https://doi.org/10.1016/j.chemgeo.2006.05.001

Kirol, A. (2023). Lake Carmi and Missisquoi Bay legacy phosphorus data. *HydroShare*. Retrieved from http://www.hydroshare.org/resource/310f417260434211bae42c2c96adedd2

Krivoruchko, K., & Gribov, A. (2019). Evaluation of empirical Bayesian kriging. *Spatial Statistics*, *32*, 100368. https://doi.org/10.1016/j.spasta.2019.100368

Laitta, M., Gabriel, M., Greeley, A., Phillips, R., D'amours, M., & Caux, P. Y. (2020). Nutrient loading and impacts in Lake Champlain – Missisquoi Bay and Lake Memphremagog. In *Lake Champlain Long-Term Water Quality and Biological Monitoring Program, 2022*.

Lemmin, U. (2020). Insights into the dynamics of the deep hypolimnion of Lake Geneva as revealed by long-term temperature, oxygen, and current measurements. *Limnology & Oceanography*, *65*(9), 2092–2107. https://doi.org/10.1002/lno.11441

Levine, S. N., Lini, A., Ostrofsky, M. L., Bunting, L., Burgess, H., Leavitt, P. R., et al. (2012). The eutrophication of Lake Champlain's northeastern arm: Insights from paleolimnological analyses. *Journal of Great Lakes Research*, *38*, 35–48. https://doi.org/10.1016/j.jglr.2011.07.007

LimnoTech. (2012). Development of a phosphorus mass balance model for Missisquoi Bay.

Lürling, M., & Mucci, M. (2020). Mitigating eutrophication nuisance: In-lake measures are becoming inevitable in eutrophic waters in The Netherlands. *Hydrobiologia*, *847*(21), 4447–4467. https://doi.org/10.1007/s10750-020-04297-9

Marsden, M. W. (1989). Lake restoration by reducing external phosphorus loading: The influence of sediment phosphorus release. *Freshwater Biology*, *21*(2), 139–162. https://doi.org/10.1111/j.1365-2427.1989.tb01355.x

Melendez-Pastor, I., Isenstein, E. M., Navarro-Pedreño, J., & Park, M.-H. (2019). Spatial variability and temporal dynamics of cyanobacteria blooms and water quality parameters in Missisquoi Bay (Lake Champlain). *Water Supply*, *19*(5), 1500–1506. https://doi.org/10.2166/ws.2019.017

Mendelsohn, D., Swanson, C., & Isaji, T. (1997). Hydrodynamic modeling of Missisquoi Bay in Lake Champlain.

Mortimer, C. H. (1941). The exchange of dissolved substances between mud and water in lakes. *Journal of Ecology*, *29*(2), 280. https://doi.org/10.2307/2256395

Müller, B., Bryant, L. D., Matzinger, A., & Wüest, A. (2012). Hypolimnetic oxygen depletion in eutrophic lakes. *Environmental Science & Technology*, *46*(18), 9964–9971. https://doi.org/10.1021/es301422r

Niemisto, J., Kongas, P., Harkonen, L., & Horppila, J. (2016). Hypolimnetic aeration intensifies phosphorus recycling and increases organic material sedimentation in a stratifying lake: Effects through increased temperature and turbulence. *Boreal Environment Research*, *21*, 571–587.

Olea, R. A. (2006). A six-step practical approach to semivariogram modeling. *Stochastic Environmental Research and Risk Assessment*, *20*(5), 307–318. https://doi.org/10.1007/s00477-005-0026-1

Orihel, D. M., Baulch, H. M., Casson, N. J., North, R. L., Parsons, C. T., Seckar, D. C. M., & Venkiteswaran, J. J. (2017). Internal phosphorus loading in Canadian fresh waters: A critical review and data analysis. *Canadian Journal of Fisheries and Aquatic Sciences*, *74*(12), 2005–2029. https://doi.org/10.1139/cjfas-2016-0500

Ostrofsky, M. L., Levine, S. N., & Lini, A. (2020). Spatial and temporal variation in sedimentary phosphorus species in Lake Champlain (Vermont, New York, Québec). *Journal of Great Lakes Research*, *46*(5), 1277–1291. https://doi.org/10.1016/j.jglr.2020.07.010

Paerl, H. W. (2014). Mitigating harmful cyanobacterial blooms in a human- and climatically-impacted world. *Life*, *4*, 988–1012. https://doi.org/10.3390/life4040988

Paerl, H. W., Havens, K. E., Xu, H., Zhu, G., McCarthy, M. J., Newell, S. E., et al. (2020). Mitigating eutrophication and toxic cyanobacterial blooms in large lakes: The evolution of a dual nutrient (N and P) reduction paradigm. *Hydrobiologia*, *847*(21), 847–4375. https://doi.org/10.1007/s10750-019-04087-y

Pettersson, K. (1998). Mechanisms for internal loading of phosphorus in lakes. *Hydrobiologia*, *373/374*, 21–25. https://doi.org/10.1023/A:1017011420035

Petticrew, E., & Arocena, J. (2001). Evaluation of iron-phosphate as a source of internal lake phosphorus loadings. *Science of the Total Environment*, *266*(1–3), 87–93. https://doi.org/10.1016/S0048-9697(00)00756-7

Porterfield, K., & Roy, E. (2021). Lake Carmi watershed phosphorus study final report.

Puttonen, I., Mattila, J., Jonsson, P., Karlsson, O. M., Kohonen, T., Kotilainen, A., et al. (2014). Distribution and estimated release of sediment phosphorus in the northern Baltic Sea archipelagos. *Estuarine, Coastal and Shelf Science*, *145*, 9–21. https://doi.org/10.1016/j.ecss.2014.04.010

R Core Team. (2021). *R: A language and environment for statistical computing*. R Foundation for Statistical Computing. Retrieved from https://www.R-project.org/

Read, J. S., Hamilton, D. P., Jones, I. D., Muraoka, K., Winslow, L. A., Kroiss, R., et al. (2011). Derivation of lake mixing and stratification indices from high-resolution lake buoy data. *Environmental Modelling & Software*, *26*(11), 1325–1336. https://doi.org/10.1016/j.envsoft.2011.05.006

Rhodes, J., Hetzenauer, H., Frassl, M. A., Rothhaupt, K.-O., & Rinke, K. (2017). Long-term development of hypolimnetic oxygen depletion rates in the large Lake Constance. *Ambio*, *46*(5), 554–565. https://doi.org/10.1007/s13280-017-0896-8

Robertson, D. M., & Diebel, M. W. (2020). Importance of accurately quantifying internal loading in developing phosphorus reduction strategies for a chain of shallow lakes. *Lake and Reservoir Management*, *36*(4), 391–411. https://doi.org/10.1080/10402381.2020.1783727

Rosa, F., & Burns, N. M. (1987). Lake Erie central basin oxygen depletion changes from 1929–1980. *Journal of Great Lakes Research*, *13*(4), 684–696. https://doi.org/10.1016/S0380-1330(87)71683-9

Samsonova, V. P., Blagoveshchenskii, Y. N., & Meshalkina, Y. L. (2017). Use of empirical Bayesian kriging for revealing heterogeneities in the distribution of organic carbon on agricultural lands. *Eurasian Soil Science*, *50*(3), 305–311. https://doi.org/10.1134/S1064229317030103

Schindler, D. W. (2012). The dilemma of controlling cultural eutrophication of lakes. *Proceedings of the Royal Society B: Biological Sciences*, *279*(1746), 4322–4333. https://doi.org/10.1098/rspb.2012.1032

Schmidt, G. (1928). Über fermentative Desaminierung im Muskel. *Hoppe-Seyler's Zeitschrift für Physiologische Chemie*, *179*(4–6), 243–282. https://doi.org/10.1515/bchm2.1928.179.4-6.243

Schroth, A. W., Giles, C. D., Isles, P. D. F., Xu, Y., Perzan, Z., & Druschel, G. K. (2015). Dynamic coupling of iron, manganese, and phosphorus behavior in water and sediment of shallow ice-covered eutrophic lakes. *Environmental Science and Technology*, *49*(16), 9758–9767. https://doi.org/10.1021/acs.est.5b02057

Schroth, A. W., Kirol, A. P., Morales-Williams, M., & Stepenuck, K. (2021). University of Vermont Lake Carmi Monitoring 2020 preliminary report to the Vermont Department of Environmental Conservation Lakes and Ponds Program.

Smeltzer, E., Shambaugh, A. D., & Stangel, P. (2012). Environmental change in Lake Champlain revealed by long-term monitoring. *Journal of Great Lakes Research*, *38*, 6–18. https://doi.org/10.1016/j.jglr.2012.01.002

Smith, L., Watzin, M. C., & Druschel, G. (2011). Relating sediment phosphorus mobility to seasonal and diel redox fluctuations at the sediment-water interface in a eutrophic freshwater lake. *Limnology & Oceanography*, *56*(6), 2251–2264. https://doi.org/10.4319/lo.2011.56.6.2251

Snortheim, C. A., Hanson, P. C., McMahon, K. D., Read, J. S., Carey, C. C., & Dugan, H. A. (2017). Meteorological drivers of hypolimnetic anoxia in a eutrophic, north temperate lake. *Ecological Modelling*, *343*, 39–53. https://doi.org/10.1016/j.ecolmodel.2016.10.014

Sobek, S., Gudasz, C., Koehler, B., Tranvik, L. J., Bastviken, D., & Morales-Pineda, M. (2017). Temperature dependence of apparent respiratory quotients and oxygen penetration depth in contrasting lake sediments. *Journal of Geophysical Research: Biogeosciences*, *122*(11), 3076–3087. https://doi.org/10.1002/2017JG003833

Søndergaard, M., Bjerring, R., & Jeppesen, E. (2013). Persistent internal phosphorus loading during summer in shallow eutrophic lakes. *Hydrobiologia*, *710*(1), 95–107. https://doi.org/10.1007/s10750-012-1091-3

Søndergaard, M., Jensen, J. P., & Jeppesen, E. (2003). Role of sediment and internal loading of phosphorus in shallow lakes. *Hydrobiologia*, *506*, 135–145. https://doi.org/10.1023/B:HYDR.0000008611.12704.dd

Sondergaard, M., Jensen, P. J., & Jeppesen, E. (2001). Retention and internal loading of phosphorus in shallow, Eutrophic Lakes. *The Scientific World Journal*, *1*, 427–442. https://doi.org/10.1100/tsw.2001.72

Song, K., Adams, C. J., & Burgin, A. J. (2017). Relative importance of external and internal phosphorus loadings on affecting lake water quality in agricultural landscapes. *Ecological Engineering*, *108*, 482–488. https://doi.org/10.1016/j.ecoleng.2017.06.008

Steinman, A., Chu, X., & Ogdahl, M. (2009). Spatial and temporal variability of internal and external phosphorus loads in Mona Lake, Michigan. *Aquatic Ecology*, *43*(1), 1–18. https://doi.org/10.1007/s10452-007-9147-6

Tammeorg, O., Nürnberg, G., Horppila, J., Haldna, M., & Niemistö, J. (2020). Redox-related release of phosphorus from sediments in large and shallow Lake Peipsi: Evidence from sediment studies and long-term monitoring data. *Journal of Great Lakes Research*, *46*(6), 1595–1603. https://doi.org/10.1016/j.jglr.2020.08.023

Trolle, D., Hamilton, D. P., Pilditch, C. A., Duggan, I. C., & Jeppesen, E. (2011). Predicting the effects of climate change on trophic status of three morphologically varying lakes: Implications for lake restoration and management. *Environmental Modelling & Software*, *26*(4), 354–370. https://doi.org/10.1016/j.envsoft.2010.08.009

U.S. EPA. (1996). Method 3050B: Acid digestion of sediments, sludges, and soils. Revision 2.

U.S. EPA. (2016). Phosphorus TMDLs for Vermont segments of Lake Champlain.

VT ANR. (2008). Phosphorus total maximum daily load (TMDL) for Lake Carmi.

VT DEC. (2020). 2019 Lake Carmi clean water progress report.

Wagner, K. J. (2017). Preface: Advances in phosphorus inactivation. *Lake and Reservoir Management*, *33*(2), 103–107. https://doi.org/10.1080/10402381.2017.1316064

Wetzel, R. G. (2001). Limnology: Lake and river ecosystems (Vol. *37*).

Wickham, H. (2016). *ggplot2: Elegant graphics for data analysis*. Springer-Verlag. ISBN 978-3-319-24277-4. Retrieved from https://ggplot2.tidyverse.org

Wilkes, A. (2019). *Phosphorus mobility and speciation under dynamic redox conditions in shallow eutrophic freshwater systems*. University of Vermont.

Winslow, L., Read, J. S., Woolway, R. I., Brentrup, J., Leach, T., Zwart, J., et al. (2019). rLakeAnalyzer: Lake physics tools (Version 1.11.4.1). Retrieved from https://cran.r-project.org/web/packages/rLakeAnalyzer/index.html

Zia, A., Schroth, A. W., Hecht, J. S., Isles, P., Clemins, P. J., Turnbull, S., et al. (2022). Climate change-legacy phosphorus synergy hinders lake response to aggressive water policy targets. *Earth's Future*, *10*(5), e2021EF002234. https://doi.org/10.1029/2021EF002234